Research Square

Preprints are preliminary reports that have not undergone peer review.
They should not be considered conclusive, used to inform clinical practice,
or referenced by the media as validated information.

Whole-Liver Automatic Function Scoring System from Gadoxetic Acid-Enhanced MRI in Predicting Post-Hepatectomy Liver Failure in Hepatocellular Carcinoma

Baodi Deng
Tongji Hospital Tongji Medical College,Huazhong University of Science and Technology
Wen Zhou
Tongji Hospital Tongji Medical College,Huazhong University of Science and Technology
Menglin Wang
Tongji Hospital Tongji Medical College,Huazhong University of Science and Technology
Robert Grimm
Siemens Healthcare GmbHSHS DI MR DL ONCO
Gen Chen
Tongji Hospital Tongji Medical College,Huazhong University of Science and Technology
Qiuxia Wang
wangqiuxia@hust.edu.cn
Tongji Hospital Tongji Medical College,Huazhong University of Science and Technology
Zhen Li
Tongji Hospital Tongji Medical College,Huazhong University of Science and Technology

Research Article

Keywords: Hepatocellular carcinoma, Hepatectomy, Post-hepatectomy liver failure, Magnetic resonance imaging, Gadoxetic Acid

Posted Date: October 29th, 2026

DOI: https://doi.org/10.21203/rs.3.rs-11121509/v1

License: This work is licensed under a Creative Commons Attribution 4.0 International License.
Read Full License

Additional Declarations: No competing interests reported.

Whole-Liver Automatic Function Scoring System from Gadoxetic Acid-Enhanced MRI in Predicting Post-Hepatectomy Liver Failure in Hepatocellular Carcinoma

Baodi Deng[1#], Wen Zhou [1#], Menglin Wang[1], Robert Grimm[2],

Gen Chen[1]*,Qiuxia Wang[1]*, Zhen Li[1]

[1]Department of Radiology, Tongji Hospital, Tongji Medical College, Huazhong University of Science and Technology.

[2]Siemens Healthcare GmbHSHS DI MR DL ONCO.

Corresponding author 1：Qiuxia Wang Email: wangqiuxia@hust.edu.cn

Corresponding author 2：Gen Chen Email:genchen@hust.edu.cn

Type of manuscript：Original Article

Abstract

Objective: This study evaluates the effectiveness of the Functional Automated Whole-Liver Score (FAWLS), derived from gadoxetic acid-enhanced MRI, in predicting post-hepatectomy liver failure (PHLF) in patients who with hepatocellular carcinoma (HCC).

Materials and Methods: A retrospective study included 183 patients who had 3-Tesla liver MRI and indocyanine green (ICG) testing for liver function evaluation between January 2022 and November 2024. PHLF was recorded according to international surgical group standard criteria. To identify independent predictors of PHLF, both univariate and multivariate binary logistic regression analyses were conducted.The diagnostic efficacy of the FAWLS parameter, ICG R15, and PHLF outcomes were assessed using ROC curves and *Delong* tests.

Result: A cohort of 129 patients (mean age 57.038±9.964; 103 males) was studied, with 34 (26.4%) developing PHLF. Univariate analysis revealed significant differences between the non-PHLF and PHLF groups in various parameters. Multivariate analysis identified the FAWLS index (OR = 0.438; $p < 0.05$) and rLV_{Liver} (OR = 0.997; $p < 0.05$) as independent predictors of PHLF. Diagnostic performance for PHLF was similar between FAWLS parameters and ICG R15 ($p > 0.05$). The combination of rLVLiver and FAWLS index had an area under the ROC curve of 0.781 (95% CI: 0.699-0.863), with 94.1% sensitivity and 50.5% specificity.

Conclusion: FAWLS index and rLV_{Liver} predict PHLF in HCC. FAWLS system predicts PHLF comparably to ICG R15. Combining rLV_{Liver} with FAWLS enhances predictive accuracy, aiding preoperative risk assessment and surgical planning.

Abbreviations

Abbreviation/Acronym	Full Name
AUC	under the curve
FLIS	functional liver imaging score
FAWLS	Functional Automated Whole-Liver Score
HCC	hepatocellular carcinoma
INR	international normalized ratio
ICG	indocyanine green

MRI	Magnetic Resonance Imaging
OR	Odds Ratio
PHLF	Post-hepatectomy liver failure
ROI	region of interest

Key words: Hepatocellular carcinoma; Hepatectomy; Post-hepatectomy liver failure; Magnetic resonance imaging; Gadoxetic Acid.

Introduction

Hepatocellular carcinoma (HCC) is one of the most common cancers in China, and it has 410,000 new cases in 2020[1]. It is second among cancer deaths and poses a serious threat to public health. Hepatectomy is currently the preferred treatment for HCC[2]. Post-hepatectomy liver failure (PHLF) is the main perioperative death cause with 4.5% to 33.7% cases[3], and when it occurs it often has severe complications such as coagulation disorders and jaundice that reduce survival rates. PHLF is closely related to lack of residual liver volume and decreased functional reserve[4]. Therefore, it is important to assess liver reserve function and residual liver to formulate surgical plans and reduce the risk of complications.

The most commonly used clinical methods for liver function assessment and prediction of PHLF have obvious limitations. Child-Pugh classification is subjective clinical measure[5]and it is difficult to quantify local functional differences of liver. Even though indocyanine green retention rate at 15 minutes (ICG R15) can accurately

measure liver excretory function[6], test results can be affected by standardization of operation, patient circulatory status, and bilirubin levels, with poor stability and reproducibility. In imaging assessment Gadoxetic acid, new type of hepatocyte specific magnetic resonance imaging contrast agent, is a new way of noninvasive liver function assessment based on enhanced MRI due to its unique properties of hepatocyte uptake and biliary excretion[7], its related functional liver imaging score (FLIS) is highly subjective and poorly reproducible[8].Although T1mapping can quantitatively assess liver function, it is impeded by two metabolic mechanisms of contrast agent distributed intravascular and extravascular spaces, and in liver cells[9]. Although the notion of hepatocyte fraction solved this problem somewhat, and more accurately reflects the uptake function of liver cells for contrast agent[10], current research methods still require manual delimitation of the region of interest (ROI) and only select some planes to analyze, and do not provide a complete estimation of the whole liver volume. In recent years several studies have shown that measurement of functional remnant liver volume using Gadoxetic Acid-enhanced MRI can predict PHLF[11].

The current study utilizes the FAWLS system in combination with deep learning based image segmentation to simulate surgical plans and obtain quantitative parameters for the liver. This methodological approach endeavors to surmount the constraints of traditional volume evaluation and enhance the accuracy of predicting PHLF in patients with HCC. The research aims to ascertain the predictive value of the FAWLS system for postoperative PHLF, offering objective indicators for liver

function prognosis. Ultimately, this strategy is designed to guide treatment decisions, thereby decreasing the incidence of PHLF and improving patient prognoses.

Graphical Abstract :The entire research process

Materials and Methods

Study Design and Participants

This research received approval from the Medical Ethics Committee of Tongji Hospital, Tongji Medical College, Huazhong University of Science and Technology (Approval No.: TJ-IRB20231133), and was conducted in accordance with the Declaration of Helsinki, with a waiver for informed consent.

Between January 2022 and November 2024, 183 consecutive patients who met the initial inclusion criteria were enrolled. Inclusion criteria were: (a) clinically suspected HCC;(b) gadoxetic acid-enhanced MRI performed within 2 weeks before surgery; (c) preoperative ICG test completed within 1 week after MRI. Exclusion criteria were : (a) age < 18 years; (b) prior transarterial chemoembolization, or targeted radiotherapy/chemotherapy within 2 weeks before MRI; (c) contraindications for contrast - enhanced MRI; (d) concurrent hepatic iron deposition or biliary obstruction. (e) history of splenectomy or liver transplantation; (f) > three malignant lesions; (g) incomplete liver coverage or poor image quality due to respiratory motion or patient intolerance. After applying exclusion criteria, 129 patients were included in the final analysis. The collected demographic information included age, gender, body mass index, and specific etiologies of liver diseases. Meanwhile, laboratory indicators

such as total bilirubin, alpha-fetoprotein, aminotransferase, and international normalized ratio were recorded.

MRI examination

All examinations were conducted utilizing a 3.0T MRI scanner (MAGNETOM Skyra, Siemens Healthcare), which was equipped with an 8-channel phased-array body coil. Before the examination, patients abstained from eating for 4 hours and participated in breathing exercises. The patients were positioned in a supine orientation, with their feet directed forward and their hands elevated above their heads.Respiratory training was conducted before the start of scanning. The scanning range extended from the superior aspect of the diaphragm to the inferior margin of the liver.Before enhancement, the standard coronal half-Fourier single-shot turbo spin-echo sequence and the transverse breath-hold three-dimensional volumetric interpolated breath-hold examination sequence were employed, and transverse T2WI sequence with diaphragm navigator combined with Blade technology were performed. The contrast agent was injected manually at a dose of 0.1 ml/kg and an injection rate of 1.0 mL/sec. After administering the contrast agent, fluoroscopic tracing was utilized to initiate a multi-phase dynamic contrast-enhanced scan, which included the early arterial phase, late arterial phase, and portal venous phase, once the contrast-medium agent reached the left ventricle. Transverse T1 mapping images were acquired using dual flip angles (3°and 15°) three-dimensional volumetric interpolated breath-hold examination before enhancement, at the delayed phase (10

min), and at the he

patobiliary phase (20 min). B1 field calibration was performed before acquisition.

Quantitative image analysis

In this study, two physicians independently performed FLIS scoring on the hepatobiliary phase images acquired at 20 min without knowing the patients' preoperative ICG R15 results. Quantitative analysis was performed using the multi-parameter analysis software (v1.2.1, Siemens Healthineers, Erlangen, Germany) developed by Siemens Medical, and was completed collaboratively by two physicians. Firstly, one physician determined the planned resection area based on the surgical record, and then another experienced physician reviewed and confirmed the resection range.

The FAWLS analysis involved four steps:

1. Data loading: Load the pre-medication T1WI, T2WI, T1 mapping, and the T1WI and T1 mapping in the hepatobiliary phase into the software.

2. Image registration: Use software to automatically register all the loaded images.

3.Automatic organ segmentation: Utilize a deep learning convolutional neural network to automatically extract and segment the entire liver volume (LV) of interest through a one-click liver segmentation button(the results are shown in Figure 2-4:a-b). By adjusting the threshold, remove the blood vessels, bile ducts of the liver, and the lesion areas for simulated surgical resection. If the segmented area (pink) is not satisfactory, perform manual modification (the results are shown in Figure 2-4:c-d).

4. Record the values: The final one-click analysis button automatically displays and records the residual liver volume (rLV_{liver}), the pre-contrast T1mapping values ($T1_{pre}liver$), the T1mapping values in the hepatobiliary phase ($T1_{HBP}liver$), the percentage change in T1mapping values (ΔT1), and the T1 values of the spleen before and after contrast enhancement. Then, calculate the FAWLS index of the residual liver using Formula 1[12](the results are shown in Figure 2-4:e-f).

$$FAWLS = \frac{\varphi spleen}{(1-\varphi liver)} \times \left(\frac{T1spleen}{T1wholeliver} - \frac{\varphi liver}{\varphi spleen}\right)$$

In this research, ΔT1 signifies the variation in T1mapping values of the remaining liver tissue before and after the administration of a contrast agent. Furthermore, φwhole liver and φspleen refer to the water content in the liver and spleen tissues, respectively[13]. These measurements were established as constants and sourced from existing literature.

As a result Gadoxetic Acid reduces the T1mapping values of the liver by being absorbed by hepatocytes and spreading in the extracellular space both within and outside blood vessels[13]. the T1mapping values of the liver is influenced by both its intracellular and extracellular elements. On the other hand, Gadoxetic acid specifically enhances the blood and extracellular regions of the spleen.Therefore, the absolute difference in the spleen T1mapping values before and after contrast agent administration (denoted as ΔT1spleen) is used as a correction factor in the calculation to account for the contrast agent effect in the intravascular and extravascular spaces[14].

ICG test

ICG clearance rate at 15 minutes (ICG-R15) was selected as a reference indicator for the preoperative assessment of liver function reserve. The ICG test was performed within 1 week after the preoperative MRI scan. Twenty milligrams of ICG was dissolved in 5ml of normal saline and injected through the peripheral vein (right cubital vein). The clearance rate of ICG was measured using a finger sensor on the instrument (iMON, Pulsion Medical Systems, Munich, Germany). An ICG-R15 <10% was considered normal[15].

Definition of PHLF

PHLF is defined by the International Study Group of Liver Surgery. It happens when the international normalized ratio (INR) is over 1.2 and bilirubin levels are above 23.0 μmol/L. This occurs on or after the fifth day after surgery, and it is not due to a blocked bile duct.[16, 17].

Statistical Analysis

Statistical analyses were performed utilizing SPSS version 27.0. Categorical variables are presented as frequencies and percentages, with group comparisons conducted using the χ^2 test.For continuous variables, data were presented as either the median (interquartile range) or the mean ± standard deviation, as appropriate. Differences between groups were evaluated using the *Mann–Whitney U* test, independent samples *t*-test, or one-way analysis of variance, depending on the data

distribution.Variables associated with PHLF at a significance level of $p < 0.05$ in univariate logistic regression were subsequently included in a multivariate binary logistic regression model to ascertain independent predictors. Spearman's rank correlation was utilized to assess the relationships between imaging parameters and preoperative ICG R15.The evaluation of discriminatory performance was conducted through receiver ROC curve analysis, with the area under the curve (AUC) serving as the primary metric.*DeLong*'s test was used for pairwise comparisons of the AUC. All statistical analyses were conducted as two-tailed tests, with a significance level set at $p < 0.05$.

Results

Demographic and clinical characteristics

After further screening, 54 cases were excluded for the following reasons: 1) poor image quality due to significant respiratory motion (n = 13); 2) a history of splenectomy or liver transplantation (n = 18); 3) large liver volume leading to incomplete scanning coverage (n = 6); 4) poor patient tolerance and inability to complete the examination (n = 7); and 5) presence of more than three malignant lesions (n = 10). Ultimately, 129 cases were included and categorized based on the ICG R15, with 80 cases showing an ICG R15 of less than 10% and 49 cases showing an ICG R15 greater than 10%. Postoperatively, 34 cases developed liver failure, comprising 22 cases with an ICG R15 greater than 10% and 12 cases with an ICG R15 of less than 10%. (see Figure 1 for the case screening process)

The study's participants had an average age of 57.03 years, with a significant majority of 79.8% (103 out of 129) being male. All subjects underwent a minor hepatectomy: 80.62% (104 out of 129) had the procedure performed openly, while 19.4% (25 out of 129) underwent laparoscopic surgery. Among these patients, 27.13% (34 out of 129) developed PHLF, whereas 72.9% (95 out of 129) experienced a positive postoperative outcome. The detailed demographic and clinical profiles of the 129 patients are showed on table1.

Correlation between quantitative parameters of FAWLS and ICG R15 Among all the parameters

ΔT1 showed a positive correlation with the ICG test, while $T1_{prep}$liver , $T1_{HBP}$liver, rLV_{liver}, FAWLS, and FLIS showed negative correlations with the ICG test. See Table 2 for details.

Univariate and multivariate binary Logistic regression analysis

Table 3 and Fig. 5 display Results derived from univariate and multivariate modeling are summarized in Table 3. According to univariate analysis, $T1_{HBP}$Liver differed significantly, ΔT1, rLV_{liver}, FLIS, ICG R15, and FAWLS index (all $p < 0.05$). However, there was no significant difference in $T1_{pre}$liver between the two groups ($p = 0.340$). Multivariate Logistic regression analysis indicated that rLV_{liver} and FAWLS index were independent predictors of PHLF ($p = 0.040$, OR = 0.997, 95% CI: 0.994, 1.000; $p = 0.043$, OR = 0.438, 95% CI: 0.197, 0.973).

Dignostic performance for predicting post-hepatectomy liver failure (PHLF)

The ROC curve was utilized to differentiate patients with PHLF from those

without. Variables with statistical significance in univariate analysis could significantly distinguish patients with or without PHLF (all $p < 0.05$). Among these parameters, the FAWLS index showed the best diagnostic performance, with an AUC value of 0.723 (95% CI: 0.636, 0.811) (Figure 6). Its sensitivity was 79.4% and specificity was 64.2%. The diagnostic model constructed with rLV_{Liver} combined with the FAWLS index had an AUC of 0.781 (95% CI : 0.699–0.863), and the corresponding sensitivity and specificity were 94.1% and 50.5%, respectively (see Table 4 for details). The *Delong* test between the AUC of ICG R15 and the FAWLS system parameters was not statistically significant (all $p > 0.05$) (see Table 5 for details).

Discussion

This prospective study demonstrates that the FAWLS system, developed using gadoxetic acid–enhanced MRI with deep learning–based automated segmentation, independently predicts PHLF in patients with HCC undergoing hepatectomy. To our knowledge, this is the first study to validate FAWLS as a noninvasive tool for preoperative risk stratification in this setting.

The essence of PHLF is that the liver reserve function is insufficient to tolerate the metabolic load after surgical trauma[18].Its core pathophysiological mechanisms involve a reduction in the effective functional volume of hepatocytes, abnormal blood perfusion, and a decline in hepatocyte regenerative capacity[19]. The core advantage of the FAWLS system lies in its ability to simultaneously capture the functional state and hemodynamic characteristics of the liver through gadoxetic acid-enhanced MRI

technology. As a liver-specific contrast agent, Gadoxetic acidcan reflect the number and functional integrity of viable hepatocytes through the process of hepatocyte uptake and excretion, and can also reflect the liver blood perfusion efficiency through its intravascular distribution characteristics[20].The correction factor of the absolute difference in spleen T1mapping values (ΔT1spleen) introduced in the FAWLS index further eliminates the interference of the difference in contrast agent distribution between intravascular and extravascular spaces on the evaluation results, making the quantification of liver function parameters closer to the real physiological state[21]. This method precisely explains the core pathological mechanism of PHLF: when the FAWLS index decreases, it indicates a decrease in the number of viable hepatocytes and insufficient liver blood perfusion. At this time, the postoperative hepatocytes cannot effectively compensate for the metabolic demand, and the risk of liver failure increases significantly[22]. This is also the key biological basis for the FAWLS index to become an independent predictor of PHLF (OR = 0.438, $p < 0.05$).

As a typical predictive indicator of PHLF, the residual liver volume signifies the liver's "structural reserve" after surgical intervention[23]. We have found that it and FAWLS together are independent predictive factors of PHLF (OR = 0.997, $p < 0.05$). Furthermore, the diagnostic model from combination of the two is more accurate (sensitivity =94.1%; specificity = 50.5%).This result shows the connection between “structural reserve” and “functional reserve” of the liver: the number of remnant liver determines the basic capacity of liver after surgery[24] and the FAWLS index reflects actual functional state of hepatocytes and blood perfusion efficiency under this

capacity. Even if the number of remnant liver is in the normal range, a low FAWLS index indicates inadequate number of functional hepatocytes or abnormal blood perfusion in remnant liver and PHLF may still occur[25]. If the FAWLS index is high, even if the number of remnant liver is slightly lower than the critical value, the high functional state of hepatocytes may compensate metabolic demand and reduce liver failure risk[26].The combined "structure + function" evaluation model more comprehensively captures the risk of PHLF than any single indicator. This broader coverage explains why its diagnostic performance exceeds that of the FAWLS system alone (AUC = 0.781) or of remnant liver volume.

In this study, the specificity of the FAWLS index combined with the rLliver index was only 50.5%. Considering the multi-factor determination mechanism of PHLF, the occurrence of PHLF is not caused by a single factor, but is jointly influenced by multiple clinical factors such as the patient's age, nutritional status, and the degree of liver cirrhosis[27]. These factors may interfere with liver reserve function and regenerative capacity through different pathways, thereby generating superposition or interaction effects among existing diagnostic indicators and weakening the specific recognition ability of a single indicator for PHLF.

Compared with the conventional ICG R15 index established in prior studies, each parameter of the FAWLS system correlates significantly with ICG R15 and offers comparable predictive power for PHLF. However, ICG R15 is susceptible to extrahepatic influences and cannot localize regional liver functional abnormalities[28].The FAWLS system, as a fully automated quantification tool,

accurately assesses local function, minimizes human error, and offers noninvasive advantages, which together enhance its clinical potential. However, the combined FAWLS–remnant liver volume model in this study attained a specificity of only 50.53%, indicating room for improvement. This limited specificity likely reflects the multifactorial etiology of PHLF, which includes factors such as age, nutritional status, and the severity of liver cirrhosis[26]. Future work should incorporate these variables to optimize the model further.

This study acknowledges several limitations. Firstly, the sample size is confined to a single center, and the incidence of PHLF is relatively low, which may reduce statistical power and limit the generalizability of the findings. Second, long-term postoperative follow-up data are lacking, preventing assessment of associations between FAWLS and long-term liver function recovery, tumor recurrence, and patient survival prognosis.

Future research should pursue three directions. First, expand the sample size and include multicenter cohorts to validate the efficacy of the FAWLS system and to clarify its clinical role. Second, conduct long-term follow-up studies to assess FAWLS for postoperative recovery monitoring and to inform adjuvant treatment decisions. Third, advance clinical translation by simplifying the FAWLS analysis software, lowering the application threshold, and improving its practical utility.it is essential to develop functional simulated resection techniques grounded in liver watershed segmentation. This approach should extend beyond the resection of the lesion alone, incorporating planning that reflects the actual liver blood flow and bile duct watershed.

Such a method can more accurately simulate the effects of surgical interventions on functional liver parenchyma, thereby enhancing the alignment between preoperative assessments and actual clinical requirements.

In conclusion, the FAWLS system, based on gadoxetic acid-enhanced MRI with automated deep learning segmentation, enables noninvasive, quantitative, and whole-liver assessment of functional reserve. The FAWLS index is an independent predictor of PHLF in patients with HCC undergoing hepatectomy, with performance comparable to ICG R15. Combining FAWLS index with residual liver volume improves predictive accuracy, supporting a combined structure–function approach for preoperative risk stratification. With further validation and technical optimization, FAWLS may become a valuable tool for personalized surgical planning and postoperative management in HCC.

Declarations

This study has received funding by National Key Research and Development Program of China (2024YFE0113500).This research received approval from the Medical Ethics Committee of Tongji Hospital, Tongji Medical College, Huazhong University of Science and Technology (Approval No.: TJ-IRB20231133), and was conducted in accordance with the Declaration of Helsinki, with a waiver for informed consent.

References

1. Bhatt A, Wu J: **Immunotherapy for recurrent hepatocellular carcinoma**. *World J Gastroenterol* 2023, **29**(15):2261–2271.
2. Zhao X, Amevor FK, Xue X, Wang C, Cui Z, Dai S, Peng C, Li Y: **Correction: Remodeling the hepatic fibrotic microenvironment with emerging nanotherapeutics: a comprehensive review**. *J Nanobiotechnology* 2023, **21**(1):152.
3. Horisberger K, Rossler F, Oberkofler CE, Raptis D, Petrowsky H, Clavien PA: **The value of intraoperative dynamic liver function test ICG in predicting postoperative complications in patients undergoing staged hepatectomy: a pilot study**. *Langenbecks Arch Surg* 2023, **408**(1):264.
4. Hall MD, Howell RM, Jackson A, Owens CA, Hernandez S, Castellino SM, Ronckers CM, Constine LS, Bradley JA: **Liver Late Effects in Childhood Cancer Survivors Treated With Radiation Therapy: A PENTEC Comprehensive Review**. *Int J Radiat Oncol Biol Phys* 2024, **119**(2):575–587.
5. Stanciu BI, Iojiban M, Morariu-Barb A, Caraiani C, Procopet B, Stefanescu H, Lupsor-Platon M: **Hepatic enhancement and signal intensity analysis on magnetic resonance imaging as prognostic biomarkers in advanced chronic liver disease**. *World J Hepatol* 2025, **17**(12):111418.
6. Zhang Q, Lei S, Zhang Q, Li Y, Xu J, Wang X, Sun S, Luo X, Peng H: **Establishment of a prognostic model for hospitalized cirrhotic patients with infection based on lumbar muscle mass**. *Heliyon* 2024, **10**(4):e25739.
7. Rushbrook SM, Kendall TJ, Zen Y, Albazaz R, Manoharan P, Pereira SP, Sturgess R, Davidson BR, Malik HZ, Manas D *et al*: **British Society of Gastroenterology guidelines for the diagnosis and management of cholangiocarcinoma**. *Gut* 2023, **73**(1):16–46.
8. Hwang JA, Min JH, Kim SH, Choi SY, Lee JE, Moon JY: **Total Bilirubin Level as a Predictor of Suboptimal Image Quality of the Hepatobiliary Phase of Gadoxetic Acid-Enhanced MRI in Patients with Extrahepatic Bile Duct Cancer**. *Korean J Radiol* 2022, **23**(4):389–401.
9. Roberts NT, Tamada D, Muslu Y, Hernando D, Reeder SB: **Confounder-corrected T(1) mapping in the liver through simultaneous estimation of T(1) , PDFF, R2* , and B1+ in a single breath-hold acquisition**. *Magn Reson Med* 2023, **89**(6):2186–2203.
10. Yoon JH, Lee JM, Kang HJ, Ahn SJ, Yang H, Kim E, Okuaki T, Han JK: **Quantitative Assessment of Liver Function by Using Gadoxetic Acid-enhanced MRI: Hepatocyte Uptake Ratio**. *Radiology* 2019, **290**(1):125–133.
11. Lauscher JC, Dixon MEB, Jada G, Afshin M, Neumann K, Cheung H, Martel G, Hallet J, Coburn N, Law C *et al*: **Prediction of post-hepatectomy liver failure by preoperative gadoxetate disodium-enhanced magnetic resonance imaging**. *HPB (Oxford)* 2024, **26**(6):782–788.
12. Yamada A, Hara T, Li F, Fujinaga Y, Ueda K, Kadoya M, Doi K: **Quantitative evaluation of liver function with use of gadoxetate disodium-enhanced MR imaging**. *Radiology* 2011, **260**(3):727–733.
13. Hu X, Li C, Wang Q, Wu X, Chen Z, Xia F, Cai P, Zhang L, Fan Y, Ma K: **Development and External Validation of a Radiomics Model Derived from Preoperative Gadoxetic Acid-Enhanced MRI for Predicting Histopathologic Grade of Hepatocellular Carcinoma**. *Diagnostics (Basel)* 2023, **13**(3).

14. Chen G, Yang B, Ma S, Chen D, Yin T, Grimm R, Wang Q, Hu X, Kamel IR, Wei L *et al*: **Quantitative assessment of liver graft function using functional automated whole-liver score derived from gadoxetic acid-enhanced MRI: a prospective cohort study**. *Int J Surg* 2025, **111**(8):5235–5244.
15. Caimano M, Bianco G, Coppola A, Marrone G, Agnes S, Lai Q, Spoletini G: **Indocyanine green clearance tests to assess liver transplantation outcomes: a systematic review**. *Int J Surg* 2024, **110**(1):431–440.
16. Lopez-Lopez V, Linecker M, Cruz J, Brusadin R, Lopez-Conesa A, Machado MA, Hernandez-Alejandro R, Voskanyan AS, Li J, Balci D *et al*: **Liver growth prediction in ALPPS - A multicenter analysis from the international ALPPS registry**. *Liver Int* 2022, **42**(12):2815–2829.
17. Wang J, Zheng T, Liao Y, Geng S, Li J, Zhang Z, Shang D, Liu C, Yu P, Huang Y *et al*: **Corrigendum: Machine learning prediction model for post- hepatectomy liver failure in hepatocellular carcinoma: a multicenter study**. *Front Oncol* 2023, **13**:1278295.
18. Nishio T, Taura K, Koyama Y, Ishii T, Hatano E: **Current status of preoperative risk assessment for posthepatectomy liver failure in patients with hepatocellular carcinoma**. *Ann Gastroenterol Surg* 2023, **7**(6):871–886.
19. Bellanti F, di Bello G, Tamborra R, Amatruda M, Lo Buglio A, Dobrakowski M, Kasperczyk A, Kasperczyk S, Serviddio G, Vendemiale G: **Impact of senescence on the transdifferentiation process of human hepatic progenitor-like cells**. *World J Stem Cells* 2021, **13**(10):1595–1609.
20. Heo S, Lee SS, Kim SY, Lim YS, Park HJ, Yoon JS, Suk HI, Sung YS, Park B, Lee JS: **Prediction of Decompensation and Death in Advanced Chronic Liver Disease Using Deep Learning Analysis of Gadoxetic Acid-Enhanced MRI**. *Korean J Radiol* 2022, **23**(12):1269–1280.
21. Arzanforoosh F, Croal PL, van Garderen KA, Smits M, Chappell MA, Warnert EAH: **Effect of Applying Leakage Correction on rCBV Measurement Derived From DSC-MRI in Enhancing and Nonenhancing Glioma**. *Front Oncol* 2021, **11**:648528.
22. Cao S, Li H, Dong S, Gao Z: **Feasibility Study of Intelligent Three-Dimensional Accurate Liver Reconstruction Technology Based on MRI Data**. *Front Med (Lausanne)* 2022, **9**:834555.
23. Wang J, Zhang Z, Shang D, Liao Y, Yu P, Li J, Chen S, Liu D, Miao H, Li S *et al*: **A Novel Nomogram for Prediction of Post-Hepatectomy Liver Failure in Patients with Resectable Hepatocellular Carcinoma: A Multicenter Study**. *J Hepatocell Carcinoma* 2022, **9**:901–912.
24. Ito Y, Hosono K, Amano H: **Responses of hepatic sinusoidal cells to liver ischemia-reperfusion injury**. *Front Cell Dev Biol* 2023, **11**:1171317.
25. Primavesi F, Maglione M, Cipriani F, Denecke T, Oberkofler CE, Starlinger P, Dasari BVM, Heil J, Sgarbura O, Soreide K *et al*: **E-AHPBA-ESSO-ESSR Innsbruck consensus guidelines for preoperative liver function assessment before hepatectomy**. *Br J Surg* 2023, **110**(10):1331–1347.
26. Rassam F, Olthof PB, Takkenberg B, Besselink MG, Busch OR, Erdmann JI, Swijnenburg RJ, van Lienden KP, Beuers UH, Bennink RJ *et al*: **Functional assessment of liver regeneration after major hepatectomy**. *Hepatobiliary Surg Nutr* 2022, **11**(4):530–538.
27. Li C, Wang Q, Zou M, Cai P, Li X, Feng K, Zhang L, Sparrelid E, Brismar TB, Ma K: **A radiomics model based on preoperative gadoxetic acid-enhanced magnetic resonance imaging for predicting post-hepatectomy liver failure in patients with hepatocellular carcinoma**. *Front Oncol* 2023, **13**:1164739.

28. Nan Y, Xu X, Dong S, Yang M, Li L, Zhao S, Duan Z, Jia J, Wei L, Zhuang H *et al*: **Consensus on the tertiary prevention of primary liver cancer**. *Hepatol Int* 2023, **17**(5):1057–1071.

Table 1. Clinical Information of Cases

Variables	Total, （n = 129）	Non-PHLF, (n = 95)	PHLF, (n = 34)	p-value
Age (years), mean ± SD	57.038±9.964	55.326±10.040	61.823±8.118	＜0.001
Gender (n, %)				0.942
Female	26(20.2%)	19(20%)	7(20.6%)	
Male	103(79.9%)	76(80%)	27(79.4%)	
BMI(kg/m²) median (IQR)	23.345(21.24,25.72)	23.39（21.30，25.73）	22.89（20.91，25.76）	0.671
Preoperative variables median (IQR)				
TBil (μmol/L)	13.80(9.70,17.60)	11.8(8.60，16.20)	16.50(13.10，27.20)	＜0.001
Albumin (g/L)	39.60(35.70，42.25)	40.10(36.70，42.80)	37.80(34.80，41.50)	0.070
ALT (U/L)	25(17，37)	22(16，34)	29.50(22，49)	0.020
AST (U/L)	33(23，48.5)	31(21，42)	49(34.50，68.75)	＜0.001
AFP (ng/mL)	15.38(3.99，164.55)	15.38(3.86，301.80)	16.59(5.06，107.08)	0.714
TBil (POD 5)	15.70(12.35，24.15)	14.80(11.60，19.90)	29.25(22.55，36.74)	＜0.001
INR(POD 5)	1.09(1.02，1.165)	1.06(1.02，1.12)	1.22(1.09，1.29)	＜0.001
ALBI grade(n,%)				＜0.001
1	67(51.9%)	57(60%)	10(29.4%)	
2	57(44.2%)	37(38.95%)	20(58.8%)	
3	5(3.9%)	1(1.05%)	4(11.8%)	
ICG graden (n,%)				＜0.001
0	79(61.2%)	67(70.5%)	12(35.3%)	
1	50(38.8%)	28(29.5%)	22(64.7%)	
Underlying diseases(n,%)				0.937
Hepatitis	97(75.2%)	72(75.8%)	25(73.5%)	
Cirrhosis	14(10.9%)	10(10.5%)	4(11.8%)	
other	18(14%)	13(13.7%)	5(14.7%)	

Footnote:BMI, body mass index; TBil, total bilirubin; ALT, alanine aminotransferase; AST, aspartate aminotransferase; AFP, alpha-fetoprotein; SD, standard deviation; IQR, interquartile range;Total bilirubin on postoperative day 5,TBil (POD 5);INR, international normalized ratioon postoperative day 5;ALBI, albumin-bilirubin; ICG-R15, indocyanine green retention rate at 15 min; PHLF, post-hepatectomy liver failure;

Continuous variables with normal distribution were expressed as mean±SD and compared using Student's t test; non-normally distributed continuous variables were expressed as median (IQR) and compared using *Mann-Whitney U* test. Categorical variables were expressed as n (%) and compared using x^2 test . Ordinal variables (ALBI grade, ICG-R15 grade) were compared using *Mann-Whitney U* test.

Table 2: Correlation Analysis of FAWLS System Parameters with ICG R15

Variables	ICG grade	
	Rho	***p*-value**
$T1_{pre}$liver (msec)	0.231	0.009
$T1_{HBP}$ liver (msec)	0.596	<0.01
ΔT1（100%）	-0.629	<0.001
rLV_{liver}	-0.366	<0.001
FAWLS	-0.511	<0.001
FLIS	-0.461	<0.001

Table 3: Results of univariate and multivariate analyses

Variables	**Non-PHLF, (*n* = 95)**	**PHLF, (*n* = 34)**	***p*-value**		**OR (95%CI)**
			Univariate	**Multivariate**	
$T1_{pre}$liver	977.84±120.75	1029.25±118.34	0.34		
$T1_{HBP}$liver	393.89 (336.92,466.19)	470.23 (392.13,532.35)	0.017		
FAWLS	2.18 (1.55,2.73)	1.57 (1.30,1.87)	＜0.001*	0.043	0.438 (0.197-0.973)
ΔT1（100%）	0.59 (0.54,0.63)	0.54 (0.50,0.60)	0.017		
rLV_{liver}	1122.70 (1022.20,1228.52)	1029.56 (902.67,1174.16)	0.002*	0.040	0.997 (0.994-1.000)
FLIS	6 (5,6)	5 (5,6)	0.003*	NA	
ICG R15(100%)	5.3% (2.9%,10.7%)	11.5% （6.8%，17.15%）	＜0.001*	NA	

Table 4: Diagnostic performance and optimal cut-off values for predicting PHLF

	AUC (95% CI)	*p*-value	Sensitivity, (%)	Specificity, (%)	Cut-off value
ICG R15(100%)	0.722(0.618,0.827)	<0.001	70.6	68.4	8.7%
$T1_{pre}$liver (msec)	0.625(0.518,0.731)	0.031	47.1	75.8	1055.28
$T1_{HBP}$ liver (msec)	0.670(0.563,0.776)	0.003	61.8	73.7	448.65
ΔT1（100%）	0.631(0.512,0.744)	0.023	53.0	74.7	54.4%
rLV_{liver}	0.669(0.560,0.778)	0.004	47.1	85.3	985.40
FAWLS	0.723(0.636,0.811)	<0.001	79.4	64.2	1.88
FLIS	0.663(0.555,0.770)	0.005	67.8	64.2	5.50
Combined diagnosis (FAWLS&rLV_{liver})	0.781(0.699,0.863)	<0.001	94.1	50.5	NA

Table 5: Paired comparison between the AUC of ICG R15 and the parameters of the FAWLS system

Variables	Difference between AUC (95% CI)	*Z*-value	*p*-value
$T1_{pre}$liver (msec)	-0.098(-0.237,0.040)	-1.390	0.165
$T1_{HBP}$liver (msec)	0.053(-0.058,0.165)	0.936	0.349
ΔT1（100%）	0.092(-0.018,0.202)	1.647	0.100
rLV_{liver}	0.053(-0.091,0.198)	0.725	0.468
FAWLS	0.001(-0.105,0.104)	-0.006	0.995
FLIS	0.060(-0.045,0.166)	1.119	0.263
Combined diagnosis (FAWLS&rL_{liver})	-0.058(-0.141,0.024)	-1.379	0.168

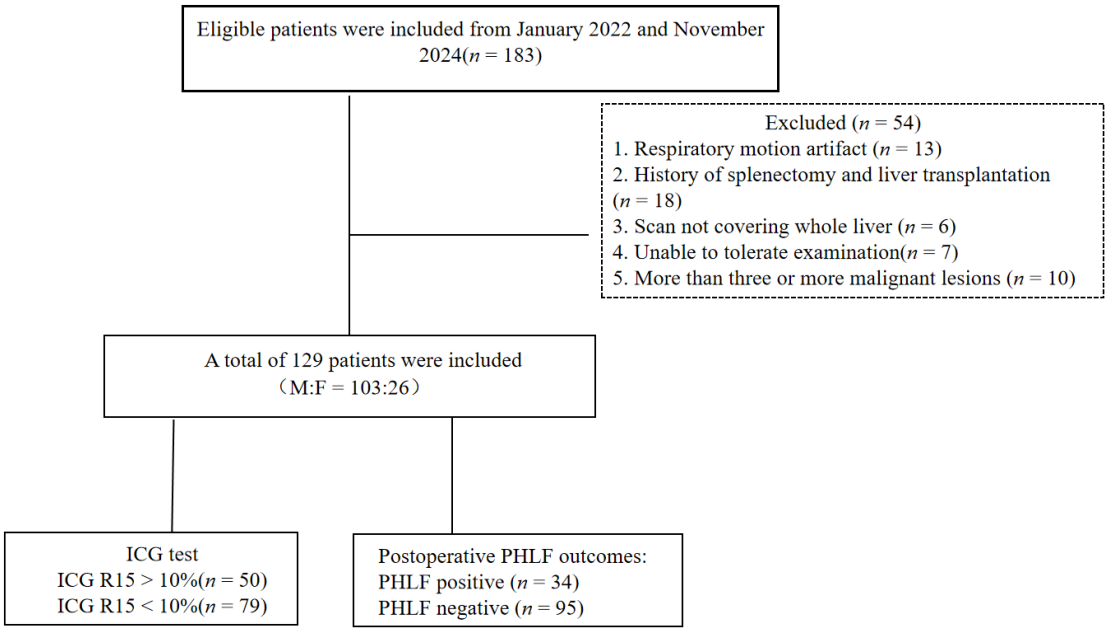


Fig. 1 Flowchart for study population enrollment

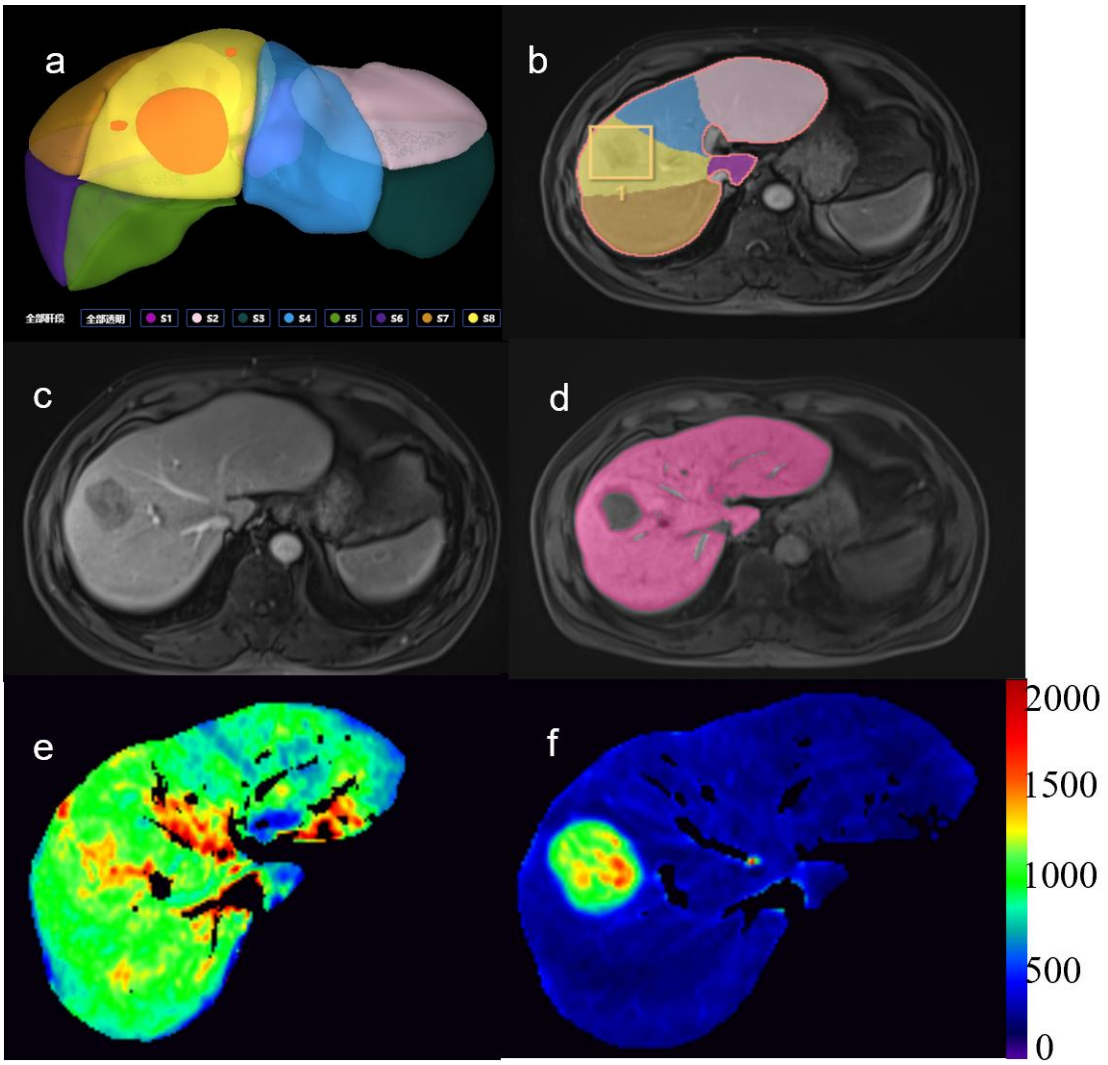


Fig. 2: Patient 1, male. ICG R15: 6.4% (<10%). During surgery, partial resection of segments 5 and 8 of the liver was performed. Liver failure occurred after the operation. The Residual liver volume was 828.60 cm^3. Before the injection of gadoxetic acid, the T1 mapping was 1131.05 ms. Twenty minutes after the injection, the T1 mapping was 488.71 ms, and the ΔT was 56.79%. The calculated FAWLS index was 1.053.

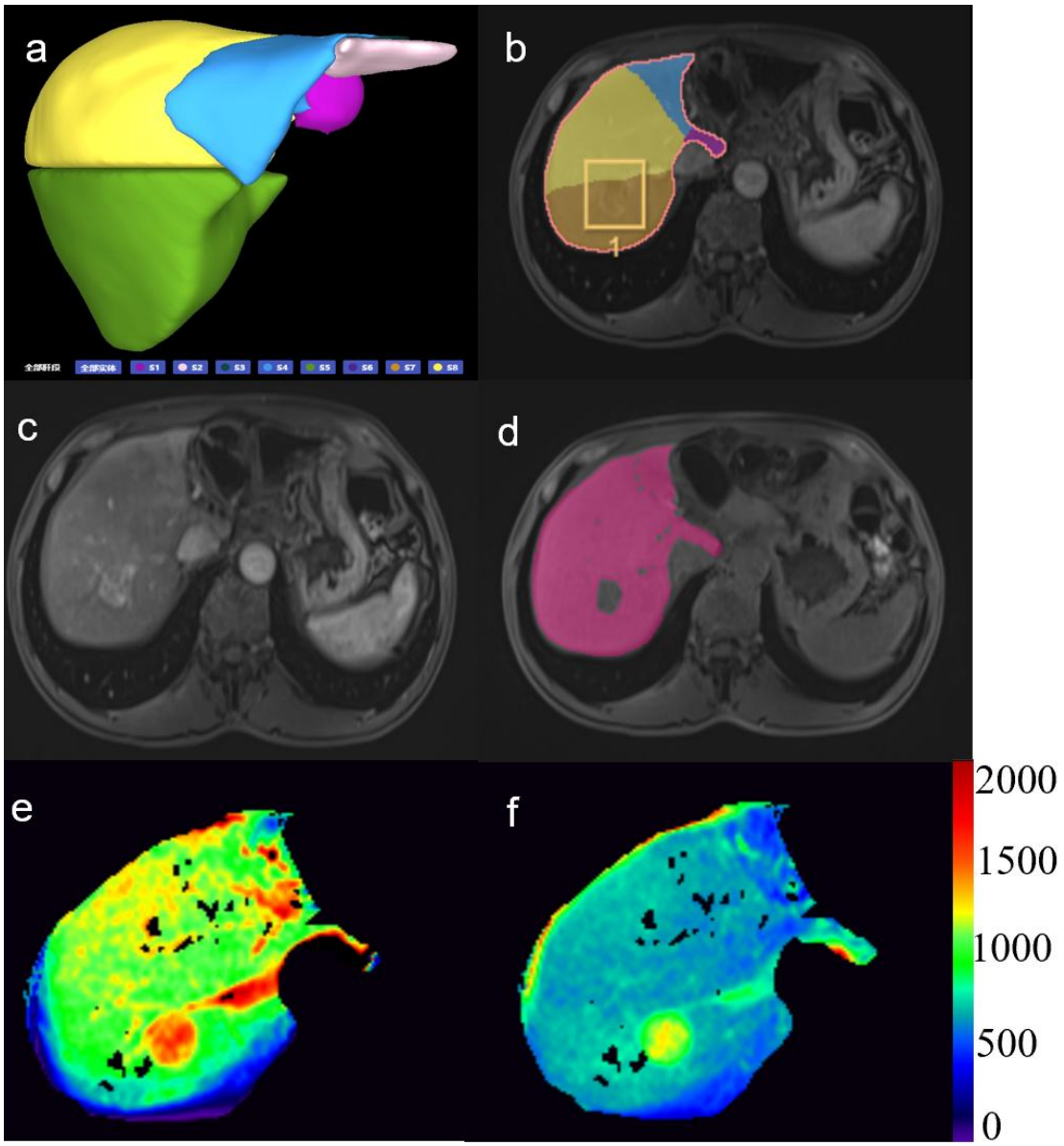


Fig. 3: Patient 2, male. ICG R18.4% (>10%). During surgery, partial resection of segments 8 of the liver was performed. No Liver failure occurred after the operation. The Residual liver volume was 988.90 cm^3. Before the injection of gadoxetic acid, the T1 mapping was 1142.30 ms. Twenty minutes after the injection, the T1 mapping was 754.41 ms, and the ΔT was 33.96%. The calculated FAWLS index was 1.900.

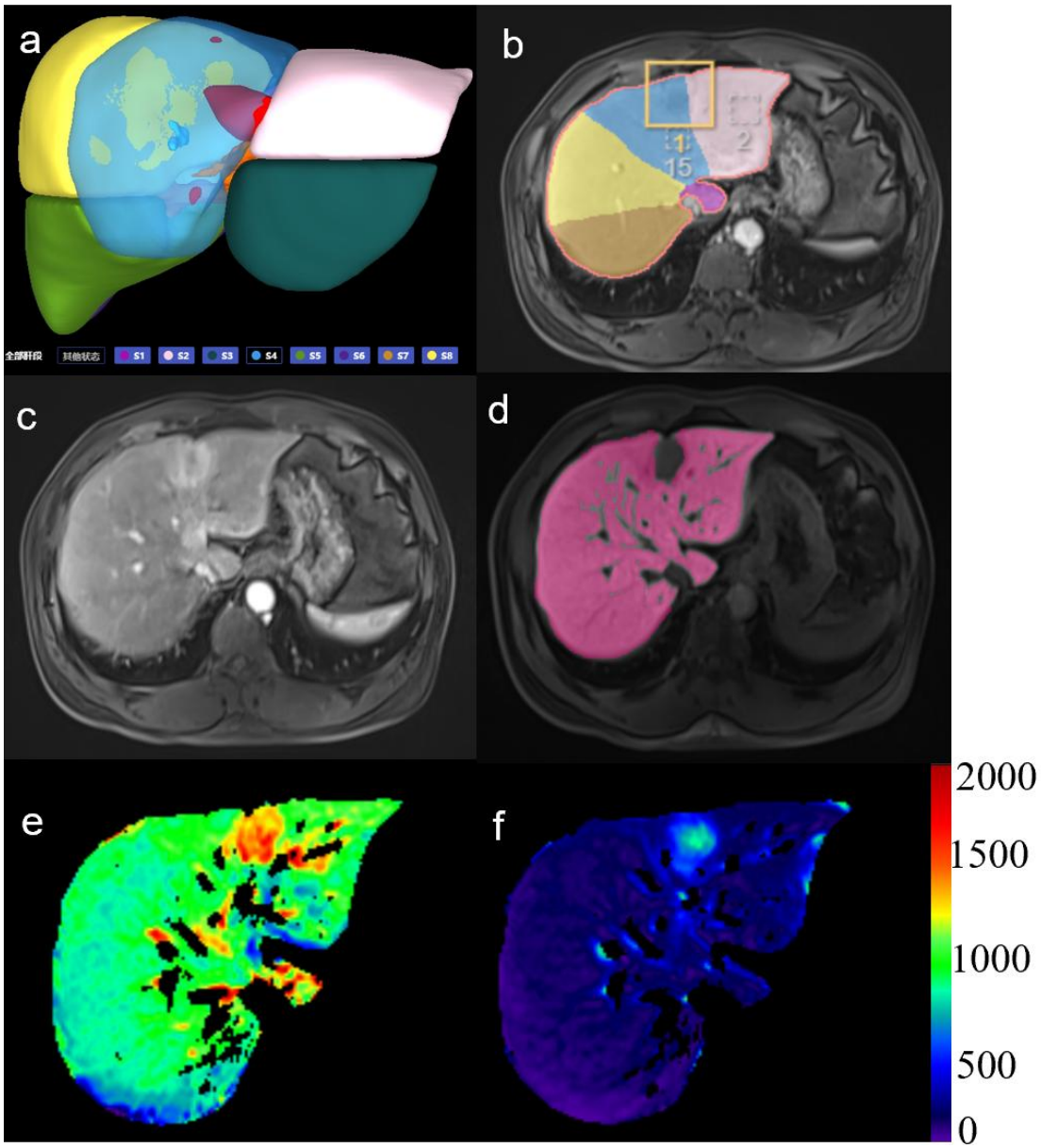


Fig. 4: Patient 3, male. ICG R5.77% (>10%). During surgery,lesions in segments 2, 3, and 4 of the liver were resected during surgery. No Liver failure occurred after the operation. The Residual liver volume was 1233.30cm³. Before the injection of gadoxetic acid, the T1 mapping was 821.43 ms. Twenty minutes after the injection, the T1 mapping was 302.96ms, and the ΔT was 63.11%. The calculated FAWLS index was 2.958.

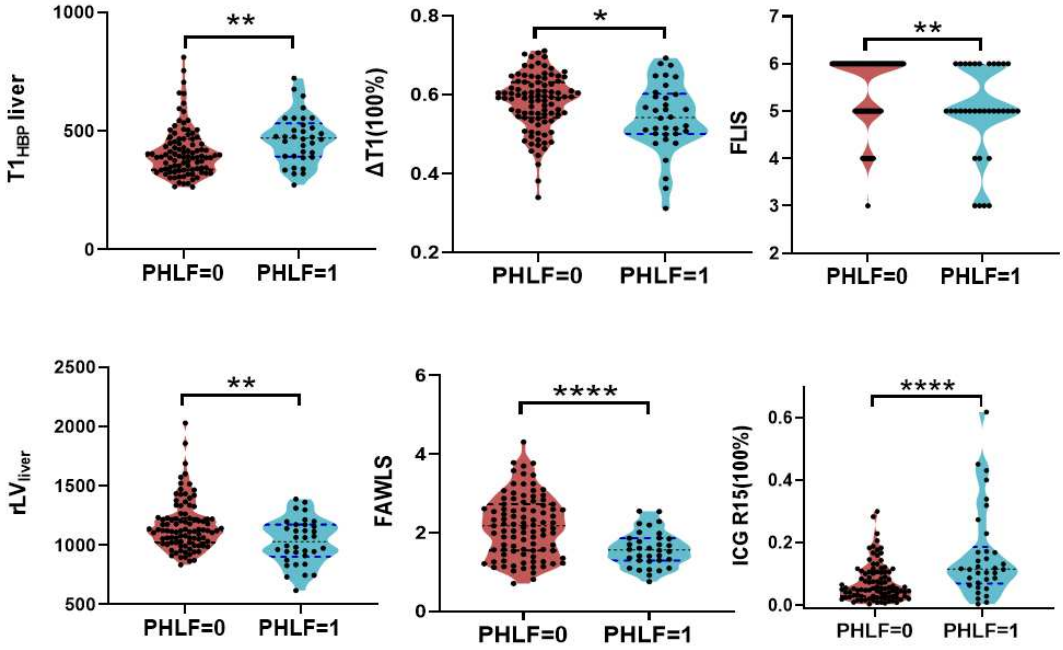


Fig. 5: Violin plot of significant differences between variables and PHLF

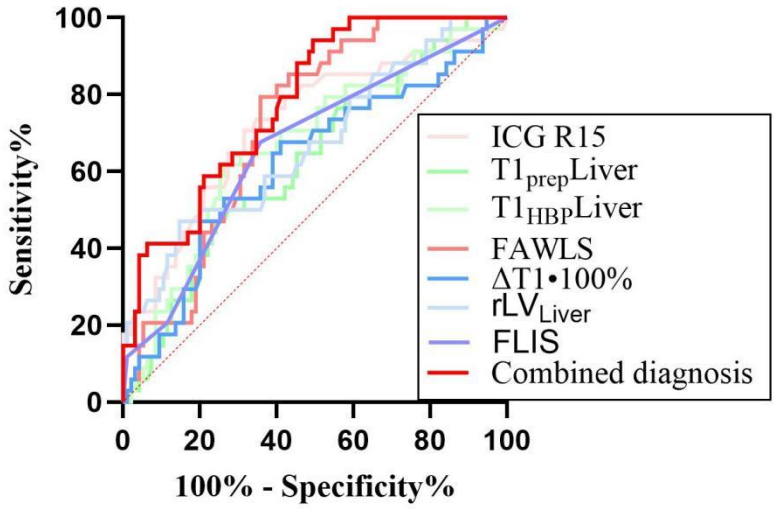


Fig. 6: ROC curve for predicting PHLF